Alexandria Engineering Journal (2016) xxx, xxx–xxx

HOSTED BY

ELSEVIER

Alexandria University

Alexandria Engineering Journal

www.elsevier.com/locate/aej
www.sciencedirect.com

ORIGINAL ARTICLE

Energy, economic and environmental performance simulation of a hybrid renewable microgeneration system with neural network predictive control

Evgueniy Entchev [a], Libing Yang [a], Mohamed Ghorab [a], Antonio Rosato [b,*], Sergio Sibilio [b]

[a] *Natural Resources Canada, CanmetENERGY, 1 Haanel Drive, Ottawa, ON K1A 1M1, Canada*
[b] *Second University of Naples, Department of Architecture and Industrial Design "Luigi Vanvitelli", via San Lorenzo, 81031 Aversa, CE, Italy*

Received 12 July 2016; revised 13 August 2016; accepted 4 September 2016

KEYWORDS

Hybrid microgeneration system;
Ground source heat pump;
Photovoltaic thermal;
Artificial neural network;
Predictive control;
Energy saving

Abstract The use of artificial neural networks (ANNs) in various applications has grown significantly over the years. This paper compares an ANN based approach with a conventional on-off control applied to the operation of a ground source heat pump/photovoltaic thermal system serving a single house located in Ottawa (Canada) for heating and cooling purposes. The hybrid renewable microgeneration system was investigated using the dynamic simulation software TRNSYS. A controller for predicting the future room temperature was developed in the MATLAB environment and six ANN control logics were analyzed.

The comparison was performed in terms of ability to maintain the desired indoor comfort levels, primary energy consumption, operating costs and carbon dioxide equivalent emissions during a week of the heating period and a week of the cooling period. The results showed that the ANN approach is potentially able to alleviate the intensity of thermal discomfort associated with overheating/overcooling phenomena, but it could cause an increase in unmet comfort hours. The analysis also highlighted that the ANNs based strategies could reduce the primary energy consumption (up to around 36%), the operating costs (up to around 81%) as well as the carbon dioxide equivalent emissions (up to around 36%).

1. Introduction

The depletion of resources as well as an environmental conscience regarding global warming have urged the need for a complete change in energy production, supply and consumption patterns in order to reduce the energy demand as well as to improve the efficiency of energy production systems

* Corresponding author. Fax: +39 081 5010845.
E-mail address: antonio.rosato@unina2.it (A. Rosato).
Peer review under responsibility of Faculty of Engineering, Alexandria University.

http://dx.doi.org/10.1016/j.aej.2016.09.001

Nomenclature

Latin letters

AC	alternating current
ANN	artificial neural network
CAD	Canadian dollar
CCHT	Canadian centre for housing technology
CO	operational cost (CAD)
CO_2	carbon dioxide
COP	coefficient of performance
CWT	cold water tank
DC	direct current
E	energy (kWh)
EER	energy efficiency ratio
FC	fuel cell
GHX	ground heat exchanger
GSHP	ground source heat pump
HVAC	heating ventilation and air-conditioning
HWT	hot water tank
MCHP	micro combined heat and power
MSE	mean squared error ($°C^2$)
OC	time percentage under "overcooling" conditions (%)
OH	time percentage under "overheating" conditions (%)
ORC	organic Rankine cycles
PEMFC	proton-exchange membrane fuel cell
PED	primary energy difference
PID	proportional-integral-derivative
PMV	predicted mean vote
PVT	photovoltaic thermal
R^2	coefficient of determination (-)
RMSE	root mean square error (°C)
SOFC	solid oxide fuel cells
SPT	solar preheat tank
T	temperature (°C)
TOU	time of use
UC	time percentage under "undercooling" conditions (%)
UH	time percentage under "underheating" conditions (%)
V	3-way valve

Greeks

Δ	difference

Superscripts

ANN	operation with artificial neural network based control strategy
on-off	operation with on-on-off control strategy

Subscripts

CWT	cold water tank
HWT	hot water tank
in	inlet
max	maximum
mean	average
OC	overcooling
OH	overheating
out	outlet
p	primary
pred	predicted by the ANN based strategies
PMV	predicted mean vote
PVT	photovoltaic thermal
room	associated with the indoor air
SPT	solar preheat tank
TRNSYS	obtained with the software TRNSYS17
UC	undercooling
UH	underheating
(+3 h)	3 h later
(+4 h)	4 h later
(+5 h)	5 h later
(+6 h)	6 h later

mainly in the residential sector (it has been estimated that buildings consume 40% of the world's energy and generate 33% of the carbon dioxide emissions [1]).

Micro-cogeneration (MCHP) systems able to produce both heat and power at the point of use (with an electric output lower than 50 kW_{el} according to [2]) are emerging as a suitable approach to reduce energy consumption and pollutant emissions by offering high efficiency and good environmental footprint, offsetting the need for centrally-generated grid electricity, enhancing energy security and avoiding transmission/distribution losses [3–6]. Today there are several technologies that are capable of providing cogeneration services [7,8] and in the recent years numerous studies have been performed on development, design guidelines, experimental testing, energy, cost and emission analyses, and optimization of MCHP systems [9,10]. Among them, the solar energy conversion into electricity and heat in a single device called photovoltaic thermal (PVT) collector is gaining an increasing attention [11–13]. This is due to the fact that the dual functions of the PVT system result in a higher overall solar conversion rate than that of solely photovoltaic or solar collectors, and thus enable a more effective use of solar energy. In addition to the micro-cogeneration technologies, several studies have recognized that the ground source heat pump (GSHP) is an efficient and environment-friendly option for space heating/-cooling of buildings [14–17] and a large number of GSHPs have been used in residential and commercial buildings throughout the world [17] mainly thanks to the advantage of using the ground or groundwater as the heat source-sink with respect to other thermal sources such as the outside air. There are several types of ground loop systems used in GSHPs, but ground-coupled heat pump systems with vertical boreholes are considered as the most suitable option for dwellings (where limited space is available) [16,17]. Combination of MCHP devices to various thermally fed or electrically-driven cooling units (such as GSHP systems) allows to set up a so-called micro combined cooling heat and power (MCCHP) system [18,19], that represents the production in situ of a threefold

Please cite this article in press as: E. Entchev et al., Energy, economic and environmental performance simulation of a hybrid renewable microgeneration system with neural network predictive control, Alexandria Eng. J. (2016), http://dx.doi.org/10.1016/j.aej.2016.09.001

energy vector requested by the user from a unique source of fuel. Although MCHP and GSHP are exciting technologies, they face several challenges, in gaining market share in mature and competitive markets, in further improving device's efficiency and reducing cost, in increasing the operational lifetime to recover the initial investment, and also in understanding the systems by both installers and potential end users.

Some authors have studied hybrid micro-cogeneration systems with the integration of geothermal or renewable sources. Gusdorf [20] reported experimental results of a residential trigeneration system using internal combustion engine and ground source heat pump. Guo et al. [21] analyzed a novel cogeneration system driven by low-temperature geothermal sources. Ribberink et al. [22] compared MCHP systems with a Stirling engine and solar collectors. Obara et al. [23] examined a completely energy-independent micro-grid consisting of photovoltaic, water electrolyzers, proton-exchange membrane fuel cell (PEMFC) and heat pumps. In [24] the model of a solar thermal cogeneration system based on organic Rankine cycle was calibrated and implemented into a larger dynamic model. Calise [25] investigated the integration of solid oxide fuel cells (SOFC) systems with solar thermal collectors. A solar heating and cooling system including photovoltaic thermal collectors was analyzed in [26,27]. Calise et al. [28] also studied polygeneration systems with PEMFC, solar heating and LiBr-H_2O absorption chiller.

Very few scientific papers have focused on the investigation of micro-cogeneration units integrated with both geothermal and renewable sources. Tempesti et al. [29,30] investigated two MCHP organic Rankine cycle (ORC) systems powered by low-temperature geothermal resources and solar energy captured by solar collectors. Entchev et al. [31] investigated the performance of an integrated ground source heat pump and natural gas fueled fuel cell (FC) microgeneration system in a load sharing application between a detached house and a small office building located in Ottawa (Canada). To continue the previous work performed by Entchev et al. [31], Yang et al. [32] investigated the performance of GSHP-FC microgeneration systems that served multiple residential and small office buildings in Ottawa (Canada) and Incheon (Republic of Korea) in order to approach real-life small neighborhood situations. Entchev et al. [33] analyzed the performance of two renewable energy systems (a GSHP system and a hybrid GSHP/PVT microgeneration system) in load sharing application between a detached house and a small office building under the climatic conditions of Ottawa (Canada). Canelli et al. [34] evaluated the energy, environmental and economic performance of two hybrid micro-cogeneration systems in a load sharing application among residential and office buildings under Naples (South Italy) weather conditions. Annex 54 of the International Energy Agency's Energy in Conservation in Buildings and Community System Programme (IEA/ECBCS) also performed an in-depth analysis of microgeneration and associated other energy technologies including, among many research activities, study of multi-source micro-cogeneration systems, polygeneration systems and renewable hybrid systems, and analysis of integrated and hybrid systems' performance when serving single and multiple residences along with small commercial premises [10]. The review of [29–34] highlights that (a) the investigation of systems composed of micro-cogeneration units integrated with both geothermal and renewable sources is of great scientific interests as well as (b) conventional on-off controllers are used to manage the systems at any case.

It is well known that the control of microgeneration systems is very important for their optimal operation and plays a key role in achieving better energy and economic performance under dynamic operating conditions. A simple on-off control strategy is still often used, but conventional controllers cannot deal with nonlinear phenomena, uncertainties of electrical and thermal demands, and time delays, and consequently they may reduce the energy efficiency and cause poor thermal comfort [35]. In fact, since building dynamic is a slow process, subject to the passively changing ambient environment, the air-conditioning systems may respond to an indoor temperature change with a significant time delay using the on-off control method since the conventional controllers cannot forecast neither the evolution of the weather conditions nor the reaction of the building under a certain weather excitation. This can lead to the so-called "overheating" (building indoor air temperature exceeding the desirable thermal comfort level) and/or "overcooling" (building indoor air temperature below the desirable thermal comfort level) despite the fact the heating/-cooling system is switched off [36–39]; if "overheating"/"over cooling" occurs then it is too late to take a control decision for the air-conditioning plant. As a result, there is a twofold negative impact causing indoor thermal discomfort and energy waste. Compared to on-off logics, proportional-integral-derivative (PID) controllers are also used as a basic control technology for system controls. However, PID controllers have limitations too: overshoot/undershoot, slow response in order to avoid oscillations, ineffective to sudden load disturbance and not suitable for systems with variable dead time and high nonlinearity. A reduction in energy consumption would have certainly been achieved if the indoor temperature trend could be forecasted in order to prevent unnecessary "overheating"/"o vercooling". Artificial neural network (ANN) is a type of artificial intelligence that mimics the behavior of the human brain. It is able to approximate a nonlinear relationship between the input and output variables of complex systems without requiring explicit mathematical representations, it can learn and reproduce the behavior of data time series, it is fault tolerant in the sense that it is able to handle noisy and incomplete data, and, once trained, it can perform predictions at very high speed. These facts provide the necessary features that an "intelligent" controller should have for achieving a rational use of energy while maintaining acceptable indoor conditions. Some papers compared the ANN approach and the PID controllers [40,41] concluding that the ANN based strategy (i) totally overcomes the disadvantages of PID controllers (such as set point changes, effect of load disturbances, processes with variable dead time) and (ii) is more responsive than PID controllers to unknown dynamics of the system which makes it even more suitable for applications having uncertainties and unknown dynamics due to environmental noise. The use of ANNs in various applications related to the energy management has been growing significantly over the years and many researchers proved that ANN-based predictive control strategies in air-conditioning applications can be very useful in optimizing the buildings' energy consumption and operating costs [35,42]. Kanarachos and Geramanis [43] designed and tested an ANN controller for managing a simple hydronic space heating system (consisting of boiler, distribution circuit and terminal units) in order to maintain the desired indoor air

Please cite this article in press as: E. Entchev et al., Energy, economic and environmental performance simulation of a hybrid renewable microgeneration system with neural network predictive control, Alexandria Eng. J. (2016), http://dx.doi.org/10.1016/j.aej.2016.09.001

temperature in a hypothetical house during two typical days. The study highlighted the capability of the ANN controller in meeting the indoor thermal comfort condition by varying the fuel mass flow or the hot water mass flow. Several architectures of the ANN controller were investigated with the best performance obtained by using the current room temperature as well as the difference between the current room temperature and the target as inputs. Argiriou et al. [44] developed an artificial neural network controller for single-family houses equipped with a simple on-off electrical heating system. The controller was used to predict the future room temperature with a time horizon of 15 min based on the current and past values of horizontal solar irradiance, external and room temperatures, as well as operating status (on or off) of the heating system. The analysis showed that a 7.5% decrease of the annual heating energy consumption could be achieved under the weather conditions of Athens (Greece) in comparison with the on-off control logic. Argiriou et al. [37] extended the above control concept proposed by Argiriou et al. [44] to a hydronic space heating system (consisting of a boiler, a distribution circuit and radiators). The current and past values of external temperature, solar irradiance, room temperature, water supply and return temperatures were used as inputs to the ANN controller. The values of solar irradiance, external temperature, room temperature, water supply and return temperatures were predicted by the ANN controller over different time horizons (1, 2 3 and 4 h). The analysis showed that the utilization of the ANN controller leads to 18% of energy savings over the test period with respect to the conventional on-off strategy under the weather conditions of Uccle (Brussels, Belgium). The use of an ANN controller for room temperature prediction over a time horizon of 8 h inside a secondary school library located in the south region of Portugal was investigated by Ruano et al. [45]. The ANN controller was used to manage an air-conditioning system during the cooling season by using the values of room temperature, solar radiation, external temperature and relative humidity, target temperature and system status (on or off) as inputs. The operation time of the air-conditioning was reduced by 27% with the ANN controller in comparison with the traditional on-off logic. A room temperature predictive control using ANN models was studied by Thomas et al. [46] by considering two small rooms: the first one heated by an electrical radiator with an adjustable power, while in the second one the room temperature was controlled by using hot/cold water pipes. The analysis was performed by varying the number and type of input signals (such as room temperature, external temperature, solar-air temperature, and water temperature) as well as the structure of the models, with prediction time horizons ranging from 10 to 30 min. Li et al. [47] applied three artificial neural networks for the prediction of the hourly cooling load of a 1120 m^2 office building in Guangzhou (China) equipped with an air-conditioning system. The external temperature and relative humidity as well as solar radiation intensity were used as inputs and the analyses highlighted the feasibility of all proposed three ANN methods in maintaining the desired room temperature. A control methodology using ANNs was formulated by Ferreira et al. [48] and applied to an existing control heating ventilation and air-conditioning (HVAC) system composed of three variable refrigerant flow systems (each one with an outdoor air cooled inverter compressor unit) in a building of the University of Algarve (south of Portugal). The room temperature, humidity and mean radiant temperature were used as inputs, while the predicted mean vote (PMV) index was assumed as output of the ANN controller. The study demonstrated that significant energy savings (greater than 50%) can be achieved thanks to the predictive controller in comparison with the traditional on-off strategy. A neural network-based model was applied to a 99.8 m^2 single-family house (equipped with a radiant floor heating system connected to a geothermal heat pump) located in Nancy (France) and then compared to conventional controllers by Salque et al. [49]. Several ANN models for room temperature predictions over the next 6 h with various sets of inputs (such as the external temperature, solar radiation, internal gains, windows opening, heating power, wind, and humidity) were developed. Over the tested month (March), energy savings with the ANN controller ranged from 6% to 17% depending on the reference logic. Huang et al. [36] proposed a new type of model predictive control scheme based on neural network feedback linearization to achieve energy-savings for the Adelaide Airport (South Australia). This approach was tested through simulations and field experiments; the results showed that the proposed method can achieve a considerable amount of savings without reducing thermal comfort when compared to the existing control scheme.

The literature review highlighted that ANNs based control logics were successfully applied mainly in the case of simple traditional heating/cooling systems. In the knowledge of the authors, the operation of complex innovative hybrid microcogeneration systems under an artificial neural network controller was never investigated; in addition, no one analyzed the potential advantages/drawbacks associated with the utilization of ANNs based strategies when applied to heating/cooling systems including one or more hot/cold water storages.

In this paper the authors performed a comparative study of an ANN based approach and conventional on-off control applied to the operation of a hybrid ground source heat pump (GSHP)/photovoltaic thermal (PVT) system (with two hot water storages and one cold water tank) serving a typical detached residential house located in Ottawa (Canada). The hybrid renewable microgeneration system was simulated in TRNSYS dynamic simulation environment (version 17) [50] also using models calibrated by the authors based on experimental data. An ANN based controller to accurately predict the room temperature over different time horizons was modeled in MATLAB environment [51] and then integrated with the developed system models in TRNSYS. Six ANN based control logics were investigated and compared to those associated with conventional on-off strategy only mainly in terms of primary energy consumption, carbon dioxide equivalent emissions as well as operating costs during two specific weeks (May 1st–May 7th and July 1st–July 7th); the ability to maintain the desired indoor comfort levels was also investigated and compared in detail to provide a better understanding of the potentiality of each strategy in limiting the overheating/overcooling phenomena as well as suggesting the best control logic to be adopted while satisfying the buildings' energy demands.

2. Description of the GSHP-PVT system

A hybrid microgeneration system, with a water-to-water ground source heat pump and photovoltaic thermal panels,

Please cite this article in press as: E. Entchev et al., Energy, economic and environmental performance simulation of a hybrid renewable microgeneration system with neural network predictive control, Alexandria Eng. J. (2016), http://dx.doi.org/10.1016/j.aej.2016.09.001

is utilized for space heating and cooling purposes and electricity demand of a detached residential house located in Ottawa, Canada (latitude: 45°24′40″ North, longitude: 75°41′53″ West). The schematic of the GSHP-PVT system is shown in Fig. 1, while the main characteristics of the system's components are reported in Table 1.

A hot water tank (HWT) with two immersed heat exchangers stores the heat provided by both the GSHP and the PVT panels for space heating during the heating season. A natural gas auxiliary heater is located at the bottom of the hot water tank to provide supplementary heat in cases where additional heat is required. A cold water tank (CWT) with an immersed heat exchanger is used to provide chilled water for space cooling during the cooling period. Both tanks have a volume of 189 L. Three-way valves are used to switch between heating and cooling loops. The 3-way valves V1 and V4 are characterized by one inlet and two outlets (diverting valves), while the 3-way valves V2 and V3 have two inlets and one outlet (mixing valves). Both the diverting and mixing valves are two-position valves: in the diverting valves, the flow is totally diverted either one way or the other, while the full flow from one or the other inlet is directed to the common outlet in the mixing valves. The hot/chilled water is delivered through pipes from the tanks to the fan-coils units installed inside the building. When there is a call for heating/cooling from the building, the blower would be on high speed; otherwise, the blower is on low speed to circulate air through the building.

Initial investigation found that use of a preheat-tank could increase the PVT energy efficiency [33]. The solar preheat heat tank has a volume of 189 L. The collected solar thermal energy is stored in the solar preheat tank (SPT) and then transferred to the hot water tank under conditions where the top temperature of the solar preheat tank is higher than the bottom of the hot water tank. The electricity produced by the PVT panels is used to meet the electric load of the building as well as to satisfy the electric requirements associated with the GSHP and auxiliaries, while electricity surplus is sold to the grid; the central electric grid is used to cover the peak demands.

The size of both HWT and CWT is selected taking into account that the typical domestic hot water storage tank volume in a single-family house in Canada is 189 L; in Drake Landing Solar Community (Okotoks, Alberta, Canada) [52], a solar preheat tank with a volume of 189 L is also used for residential applications. Therefore all three tanks are chosen as 189 L.

The water-to-water heat pump, thermally interacting with the ground by means of a ground heat exchanger (GHX), has two stages considering the high heating and low cooling demands in Ottawa. The GSHP considered in this study is the model WT036 (GL) commercialized by the company ENERTECH [53]; it is characterized by maximum and minimum heating capacities equal to 10.5 kW and 7.0 kW, respectively, while the maximum and minimum cooling capacities are equal to 7.0 kW and 5.3 kW, respectively. Depending on the entering source and load water temperatures, its nominal heating Coefficient Of Performance (COP) ranges from 2.3 to 6.7, while its nominal Energy Efficiency Ratio (EER) during the cooling season ranges from 2.8 to 8.3 based on the manufacturer's performance data. In particular, the nominal heating COP at reference conditions (entering source water temperature of 0 °C and entering load water temperature of 40 °C) is equal to 3.1, while the nominal EER at reference conditions (entering source water temperature of 25 °C and entering load water temperature of 12 °C) is 20.6 [54]. The borehole field

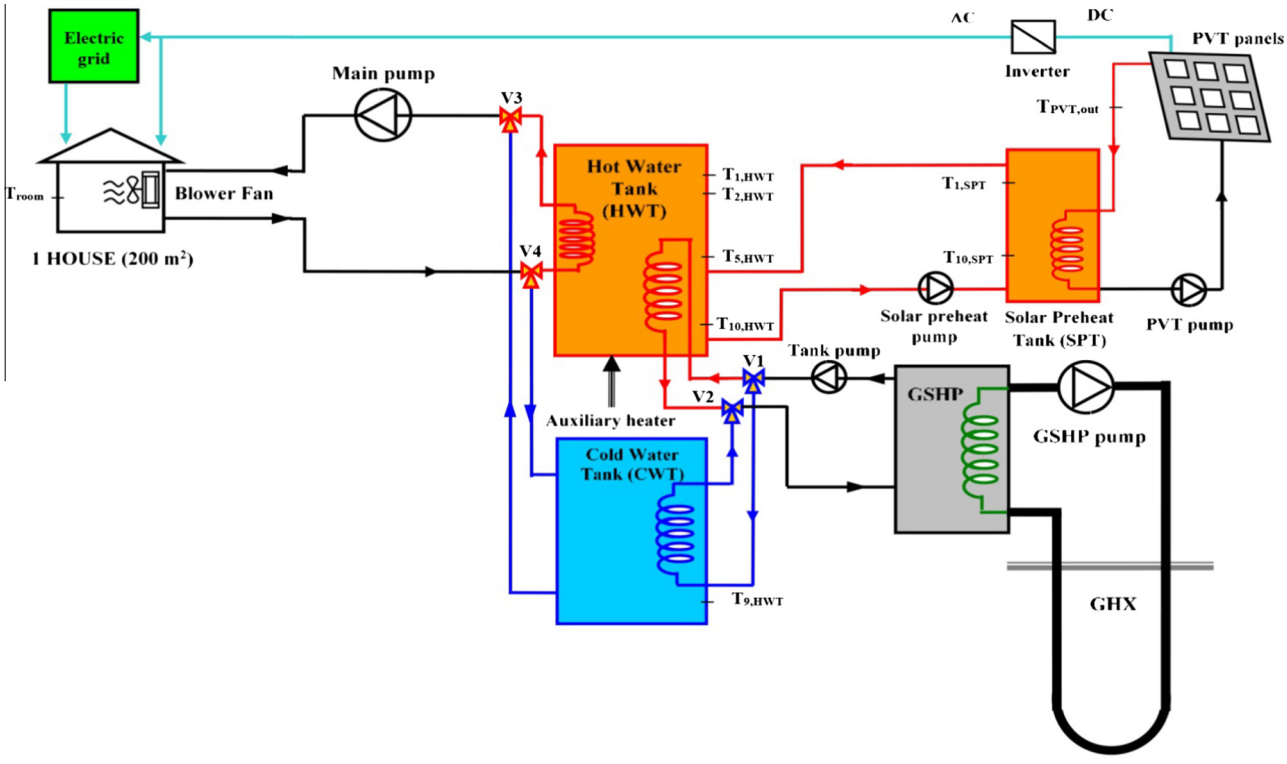

Figure 1 Schematic of the GSHP/PVT system.

Table 1 Main input parameters for the reference GSHP-PVT system.

Hot Water Tank	Volume (L)	189
	Number of immersed heat exchangers	2
Cold Water Tank	Volume (L)	189
	Number of immersed heat exchangers	1
Solar Preheat Tank	Volume (L)	189
	Number of immersed heat exchangers	1
Auxiliary heater	Auxiliary heater capacity (kW)	35
	Fuel	Natural gas
Pumps	Rated flow of GSHP pump (kg/h)	1800
	Rated power of GSHP pump (W)	180
	Rated flow of tank pump (kg/h)	2000
	Rated power of tank pump (W)	200
	Rated flow of main pump (kg/h)	1000
	Rated power of main pump (W)	100
	Rated flow of PVT pump (kg/h)	540
	Rated power of PVT pump (W)	54
	Rated flow of solar preheat pump (kg/h)	120
	Rated power of Solar preheat pump (W)	50
Heating & Cooling Coils	Air flow at high fan speed (kg/h)	1943.3
	Air flow at low fan speed (kg/h)	511.4
	Blower fan power (high)	325
	Blower fan power (low)	50
Ground Source Heat Pump (GSHP)	Rated high heating capacity (kW)	10.5
	Rated low heating capacity (kW)	7.0
	Rated high cooling capacity (kW)	7.0
	Rated low cooling capacity (kW)	5.3
Ground Heat Exchanger (GHX)	Number of boreholes	2
	Borehole depth (m)	80
	Borehole storage volume (m^3)	1698
	Soil thermal conductivity (W/m K)	2.7
	Soil heat capacity (kJ/m^2 K)	2160
	Soil thermal diffusivity (m^2/s)	$1.25\dot{s}10^{-6}$
	Outer radius of U-tube pipe (m)	0.01664
	Inner radius of U-tube pipe (m)	0.01372
	Borehole radius (m)	0.1016
	U-tube pipe thermal conductivity (W/m K)	0.42
	Grout thermal conductivity (W/m K)	1.3
PVT system	Number of panels	15
	Aperture area of a single panel (m^2)	2.95
	Rated electrical capacity of a single panel (W)[a]	295
	Rated thermal capacity of a single panel (W)[a]	1535

[a] At incident solar radiation of 1000 W/m^2 and ambient temperature of 25 °C.

contains two 80-m deep vertical ground heat exchangers with a total borehole storage volume of 1698 m^3.

There are 15 flat PVT panels with serpentine copper tubes. Each PVT panel (with aperture area of 2.56 m^2) has an electric power output of 295 W and a thermal power of 1535 W rated by the manufacturer at incident solar radiation of 1000 W/m^2 and ambient temperature of 25 °C. The solar collectors are installed assuming a tilt angle of 45° (according to the latitude of Ottawa) and an azimuth angle of 0° with water flowing through the panels array.

The building is a square shaped one story detached house with a floor area of 200 m^2 and an attic. The floor to ceiling height is 2.7 m, while the attic's height is 1.5 m. The window to wall area ratio is fixed at 35%. The building specifications meet the building envelope requirements recommended by ASHRAE Standard 90.1-2007 [55]. The overall heat transfer coefficient has value of 0.27, 0.43, 0.934 and 3.12 $W/(m^2 K)$ for roof, external wall, floor and windows respectively. The solar heat gain coefficient for the windows has a value of 0.40. This kind of building is investigated mostly because it is very common in Ottawa.

The GSHP-PVT system was modeled and implemented in TRNSYS (version 17) [50]. It is one of the most popular advanced dynamic building energy simulation programs; it has a modular structure and each component of the system is modeled by means of subroutines ("types"). In the present study, the component models were selected from the TRNSYS libraries and enhanced with latest manufacturers' systems performance data. Brief descriptions are given for some of the components in the following.

Please cite this article in press as: E. Entchev et al., Energy, economic and environmental performance simulation of a hybrid renewable microgeneration system with neural network predictive control, Alexandria Eng. J. (2016), http://dx.doi.org/10.1016/j.aej.2016.09.001

Hot/cold water storage tanks are modeled as vertical ones with immersed coiled tube heat exchangers ("Type 534"). In the hot water storage tank, the immersed heat exchanger delivering heat to the tank is located near the bottom, while the immersed heat exchanger for the heating coil is near the top. For the cold water storage tank, the immersed heat exchanger was assumed to be located near the top. Both storage tanks are assumed to be located inside of the building with a surrounding temperature of 20 °C. The TRNSYS tank model requires entering heat loss coefficient for top, bottom and edge, respectively [56]: it is assumed that the edge heat loss coefficient is 1.3 kJ/(h m^2 K), while the top/bottom heat loss coefficient is 5.0 kJ/(h m^2 K) according to the usual storage tank insulation in Canada market.

The water-to-water ground source heat pump is modeled through the "Type 668". This model relies upon catalogue data readily available from heat pump manufacturers [53,54].

The "Type 557a" is used in order to model the vertical ground heat exchanger (single U-tube). The design of the GHX is based on German guideline for ground source heat pumps (VDI 4640 [57]). The model assumes that the boreholes are placed uniformly within a cylindrical storage volume of ground; there is convective heat transfer within the pipes, and conductive heat transfer to the storage volume.

The "Type 563" is used to model the PVT panels. This model relies on linear factors relating the efficiency of the PV cells to both cell temperature and incident solar radiation. In this paper the "Type 563" model was validated by the manufacturer specification and experimental data obtained from [58]. In particular, the efficiency of PV cells in converting incident solar radiation to electricity at reference conditions (incident solar radiation of 1000 W/m^2 and ambient temperature of 25 °C) was found equal to 12%. The results showed a good agreement (with a difference less than 10%) between the simulated and experimental data for the PVT electric power and energy efficiency. The maximum fluid temperature at the outlet of PVT panels is set at 70 °C; in the case of the outlet temperature exceeds the limit, the thermal energy surplus is dissipated through a dry cooler.

The blower is modeled as a two-speed one ("Type 644") which is able to spin at one of two speeds (high and low), thereby maintaining one of two constant mass flow rates of air.

Both the heating coil model ("Type 753") and the cooling coil model ("Type 508") use a by-pass fraction approach. In this study the fraction of air unaffected by the coil that is remixed with the air stream passing through the coil is assumed equal to zero.

The residential house and related thermal loads are simulated using the interface "TRNBuild" of TRNSYS and its "Type 56". A single interior zone is assumed in the simulations. An overhang shading device was modeled through the "Type 34" in order to reduce the solar gain in the cooling period.

The house internal gain schedule is based on the Canadian centre for housing technology (CCHT) [59] simulated gains generated by a family of four persons, light bulbs, house appliances and heating equipment [60]. The total internal gain is 13.22 kW h/day. The moisture generation sources are from humans, cooking, shower, bath, cloth washer, dishwasher, mopping, plants, etc. The total moisture generation is 7.6 kg/day [55].

Non-HVAC electric loads are the ones not related to HVAC system operation. In the present study, the non-HVAC electrical load profile is based on the one at the CCHT characterized by a total electricity consumption of 5047 kW h/year, which is used by lighting, stove, kitchen products and fan, refrigerator, dishwasher, cloth washer and dryer. It was scaled up to achieve an annual consumption close to the Canadian "average" usage value [61] at 8001 kW h/year.

Annual space heating and cooling intensities are equal to 111.9 kW h/m^2-year and 22.6 kW h/m^2-year, respectively. Space heating load accounts for the largest share of the total load, and then followed by the non-HVAC electric and space cooling loads. The building model was calibrated by CCHT measured annual heating and cooling loads in 2003, with difference less than 2% between the simulated and measured ones.

The circulation pumps were modeled as two-speed pumps ("Type 656") that are able to maintain constant outlet mass flow rate between zero and a rated value taking into account that an on-off control is generally used for regulating the flow rate of pumps (instead of a fully modulated strategy).

Other component models used the manufacturers' catalogue data or validated by their specifications.

The simulation models were run under the Ottawa (Canada) weather conditions from the Canadian weather for energy calculations database in EnergyPlus format [62].

3. Control strategies

In this work several control strategies based on the utilization of artificial neural networks were developed and compared with a conventional on-off logic. In the following two paragraphs, the main characteristics of both the ANN based approaches as well as the on-off controllers are described in detail.

3.1. On-off control strategy

TRNSYS software (version 17) [50] is used for the implementation of the on-off controllers of the GSHP-PVT system.

Table 2 shows the implemented on-off control logic of the GSHP/PVT system and it components.

With this strategy, the GSHP, the tank pump and the GSHP pump are controlled by an aquastat ("Type 2") located in both the hot water tank and the cold water tank depending on the temperature level at two different layers/nodes. Both tanks are modeled with 10 isothermal temperature layers to better represent the stratification in the tank, where the top layer is 1 and the bottom layer is 10. The parameters T_2, T_5 and T_9 in Table 2 indicate the temperature sensor locations in the tank layers. Even if a two-stage GSHP was selected in this study, this component was never operated at its lower heating/cooling capacity under the on-off control logic.

During the heating period the GSHP, the tank pump and the GSHP pump would be turned on if the upper layer temperature $T_{2,HWT}$ falls below 50 °C and then turn off when the lower layer temperature $T_{5,HWT}$ approaches its set point (55 °C); during the cooling period the GSHP, the tank pump and the GSHP pump would be turned off if the temperature $T_{9,CWT}$ approaches its set point (9 °C) and then turn on when the temperature $T_{9,CWT}$ becomes larger than 15 °C.

Please cite this article in press as: E. Entchev et al., Energy, economic and environmental performance simulation of a hybrid renewable microgeneration system with neural network predictive control, Alexandria Eng. J. (2016), http://dx.doi.org/10.1016/j.aej.2016.09.001

Table 2 On-off control logic of the GSHP-PVT system.

	Monitored parameters	ON	OFF
Operation of *GSHP* during cooling season	$T_{9,CWT}$	$T_{9,CWT} \geqslant 15$ °C (high cooling capacity)	$T_{9,CWT} \leqslant 9$ °C
Operation of *GSHP* during heating season	$T_{2,HWT}$, $T_{5,HWT}$	$T_{2,HWT} \leqslant 50$ °C (high heating capacity)	$T_{5,HWT} \geqslant 55$ °C
Operation of *tank pump* and *GSHP pump* during cooling season	$T_{9,CWT}$	$T_{9,CWT} \geqslant 15$ °C	$T_{9,CWT} \leqslant 9$ °C
Operation of *tank pump* and *GSHP pump* during heating season	$T_{2,HWT}$, $T_{5,HWT}$	$T_{2,HWT} \leqslant 50$ °C	$T_{5,HWT} \geqslant 55$ °C
Operation of *auxiliary heater* during heating season	$T_{2,HWT}$, $T_{5,HWT}$	$T_{2,HWT} \leqslant 45$ °C	$T_{5,HWT} \geqslant 50$ °C
Operation of *blower fan* and *main pump* during cooling season	T_{room}	$T_{room} \geqslant 25.5$ °C	$T_{room} < 24.5$ °C
Operation of *blower fan* and *main pump* during heating season	T_{room}	$T_{room} \leqslant 20.5$ °C	$T_{room} > 21.5$ °C
Operation of *PVT pump*	$T_{PVT,out}$, $T_{1,SPT}$, $T_{10,SPT}$	$(T_{PVT,out} - T_{10,SPT}) \geqslant 10$ °C & $T_{1,SPT} \leqslant 70$ °C	$(T_{PVT,out} - T_{10,SPT}) \leqslant 3$ °C or $T_{1,SPT} > 70$ °C
Operation of *solar preheat pump*	$T_{1,SPT}$, $T_{1,HWT}$, $T_{10,HWT}$	$(T_{1,SPT} - T_{10,HWT}) \geqslant 7$ °C & $T_{1,HWT} \leqslant 70$ °C	$(T_{1,SPT} - T_{10,HWT}) \leqslant 2$ °C or $T_{1,HWT} > 70$ °C
Operation of *room thermostat* during heating season	T_{room}	$T_{room} \leqslant 20.5$ °C	$T_{room} \geqslant 21.5$ °C
Operation of *room thermostat* during cooling season	T_{room}	$T_{room} \geqslant 25.5$ °C	$T_{room} \leqslant 24.5$ °C

The natural gas-fired auxiliary heater located at the bottom of the hot water storage tank is controlled depending on the temperatures $T_{2,HWT}$ and $T_{5,HWT}$ of the hot water tank during the heating season.

A single level differential controller was used to model the room thermostat. The "Type 671" and "Type 672" are used to simulate the thermostat in both heating and cooling modes, respectively. As highlighted in Table 2, the room thermostat set point is set up at 21.0 °C during the heating period and 25.0 °C during the cooling period with a dead-band of 1.0 °C. This allows maintaining the room temperature within the range of 20.5–21.5 °C during the heating season and 24.5–25.5 °C during the cooling season. The blower fan and main pump are controlled by the temperature difference between the actual room temperature T_{room} and thermostat set point. The "Type 647" is used to simulate the operation of the 3-way diverting valves V1 and V4, while the 3-way mixing valves V2 and V3 are modeled by using the "Type 649". The valves V3 and V4 direct the hot/cold water flow from the tanks toward the building and vice versa in the case of both the main pump and blower fan are activated; the valves V1 and V2 direct the hot/cold water flow from the GSHP toward the tanks and vice versa when the tank pump being on.

The operation of the PVT pump is dependent on the temperature at the outlet of the PVT panels $T_{PVT,out}$ as well as the temperatures $T_{1,SPT}$ and $T_{10,SPT}$ in the layers 1 and 10, respectively, of the solar preheat tank (10 isothermal temperature layers were considered in the model with the layer 1 at the top and the layer 10 at the bottom). The pump is on and start to circulate fluid to all PVT panels when $T_{PVT,out}$ is at least 10 °C higher than $T_{10,SPT}$ together with $T_{1,SPT} \leqslant 70$ °C. It stops when the temperature difference is less than 3 °C or $T_{1,SPT}$ becomes larger than 70 °C. The solar preheat tank pump circulates water between the solar preheat tank and the hot water storage tank. It is controlled similar to the PVT pump depending on the temperature at layer 1 of the solar preheat tank $T_{1,SPT}$ as well as the temperatures $T_{1,HWT}$ and $T_{10,HWT}$ in the layers 1 and 10, respectively, of the hot water tank.

All the temperatures (listed in Table 2) monitored to select the on-off operation logic are indicated in the scheme in Fig. 1, identifying the position close to the possible measurement points.

3.2. Artificial neural network-based control strategies

The MATLAB® (The MathWorks Inc.) Neural Networks Toolbox [63] is used for the implementation of the artificial neural network based controllers.

The ANN architecture usually consists of three parts operating in parallel: 1 input layer, 1 or more hidden layers and 1 output layer. Each layer contains a number of neurons, with the neurons in one layer being connected to all the neurons of the previous and subsequent layers. Each connection between two neurons is associated with an adaptable synaptic weight and bias; using a suitable learning method, the neural networks are trained so that a particular input leads to a specific target output by adjusting the weights and biases (typically, many such input/target pairs are needed to train a neural network). The training process continues until the error between the network output and the desired target falls below a predetermined tolerance or the maximum number of iterations (epochs) is reached.

In this study 8 different artificial neural networks (four ANNs to be used during the heating period and four ANNs to be used during the cooling period) were trained. Table 3 reports the outputs and the inputs associated with the 8 ANNs developed in this study for both the heating period (ANNH1, ANNH2, ANNH3, ANNH4) and the cooling period (ANNC1, ANNC2, ANNC3, ANNC4). Each ANN has 1 input layer with 11 neurons, 2 hidden layers with 20 neurons

Please cite this article in press as: E. Entchev et al., Energy, economic and environmental performance simulation of a hybrid renewable microgeneration system with neural network predictive control, Alexandria Eng. J. (2016), http://dx.doi.org/10.1016/j.aej.2016.09.001

per each hidden layer and 1 output layer with 1 neuron. Each network has 1 output neuron because there is only 1 target value associated with each 11-elements input vector.

Each artificial neural network was trained in order to predict the room temperatures over different time horizons. The following 4 outputs were assumed for the 4 ANNs to be used during heating season and the 4 ANNs associated with the cooling season:

- room temperature 3 h later the current $T_{room,(+3h)}$;
- room temperature 4 h later the current $T_{room,(+4h)}$;
- room temperature 5 h later the current $T_{room,(+5h)}$;
- room temperature 6 h later the current $T_{room,(+6h)}$.

Considering that a controller to be widely used must be reasonably priced, it has to have the strict minimum of input requirements. The number and type of the inputs were selected also on the basis of the results of previous studies available in the current literature [37,44]. Accordingly, the selected input parameters for the new ANN-based controller include the following:

- the current, past and future ambient temperature;
- the current, past and future solar irradiance (on a horizontal surface);
- the current, past and future internal gains (generated by persons, light bulbs and house appliances);
- the current and past room temperatures.

The hyperbolic tangent sigmoid transfer function (“tansig”) was used in the hidden layers and the linear transfer function (“purelin”) was applied in the output layer as the two-layer sigmoid/linear network usually can represent any functional relationship between the inputs and outputs if the sigmoid layer has enough neurons. Levenberg-Marquart back-propagation training algorithms (“trainlm”) were used as a training function to update the weight and bias values, since it is the fastest training algorithm for networks of moderate size although it can require additional memory [63].

The data required for training, testing and validation of the ANNs were obtained by simulating the GSHP-PVT with the traditional on-off control under the climatic conditions of Ottawa using TRNSYS 17. Two different data sets (composed of 3840 data points in total) were extracted from the simulations results obtained only during the heating season: the first data set was used for training purposes, while the second one was considered for testing and validation of the networks ANNH1, ANNH2, ANNH3 and ANNH4. Two additional data sets (composed of 3840 data points in total) were extracted from the data obtained with TRNSYS 17 only during the cooling period: the first data set was used for training purposes, while the second one was considered for testing and validation of the networks ANNC1, ANNC2, ANNC3 and ANNC4.

The values predicted by the ANN models were compared to the entire data set (including training, testing and validation data) in terms of coefficient of determination (R^2), mean squared error (MSE) and root mean square error (RMSE). The values of MSE, R^2 and RMSE were calculated using the following formulas:

$$R^2 = 1 - \left[\sum_{i=1}^{N}\left(T_{room,TRNSYS,i} - T_{room,pred,i}\right)^2 \Big/ \sum_{i=1}^{N}\left(T_{room,TRNSYS,i} - \bar{T}_{room,TRNSYS}\right)^2\right] \quad (1)$$

$$MSE = (1/N)\sum_{i=1}^{N}\left(T_{room,TRNSYS,i} - T_{room,pred,i}\right)^2 \quad (2)$$

$$RMSE = \sqrt{(1/N)\sum_{i=1}^{N}\left(T_{room,TRNSYS,i} - T_{room,pred,i}\right)^2} \quad (3)$$

where $T_{room,TRNSYS}$ is actual room temperature provided by TRNSYS 17, $\bar{T}_{room,TRNSYS}$ is the mean of the values from TRNSYS 17, $T_{room,pred}$ is the room temperature predicted by ANN models and N is the number of data points.

Table 4 summarizes the values of R^2, MSE and RMSE associated with the ANNs developed in this study. The errors

Table 3 Architecture of the 8 artificial neural networks.

Name	ANNs to be used during heating period				ANNs to be used during cooling period			
	ANNH1	ANNH2	ANNH3	ANNH4	ANNC1	ANNC2	ANNC3	ANNC4
Output	$T_{room,(+3h)}$	$T_{room,(+4h)}$	$T_{room,(+5h)}$	$T_{room,(+6h)}$	$T_{room,(+3h)}$	$T_{room,(+4h)}$	$T_{room,(+5h)}$	$T_{room,(+6h)}$
1st input	Current ambient temperature							
2nd input	Ambient temperature 7.5 min before							
3rd input	Ambient temperature 3 h later	Ambient temperature 4 h later	Ambient temperature 5 h later	Ambient temperature 6 h later	Ambient temperature 3 h later	Ambient temperature 4 h later	Ambient temperature 5 h later	Ambient temperature 6 h later
4th input	Current solar irradiance							
5th input	Solar irradiance 7.5 min before							
6th input	Solar irradiance 3 h later	Solar irradiance 4 h later	Solar irradiance 5 h later	Solar irradiance 6 h later	Solar irradiance 3 h later	Solar irradiance 4 h later	Solar irradiance 5 h later	Solar irradiance 6 h later
7th input	Current internal gains							
8th input	Internal gains 7.5 min before							
9th input	Internal gains 3 h later	Internal gains 4 h later	Internal gains 5 h later	Internal gains 6 h later	Internal gains 3 h later	Internal gains 4 h later	Internal gains 5 h later	Internal gains 6 h later
10th input	Current room temperature							
11th input	Room temperature 7.5 min before							

reported in the table are very small and show clearly the ability of the ANNs to predict the future values of room temperature.

A detailed sensitivity analysis was performed in order to finalize the architecture of the selected ANNs. Taking into account that more neurons allow the network to solve more complicated problems and more hidden layers might result in the network solving complex problems more efficiently (even if they require more computation) [63], a number of ANN networks consisting of 1 and 2 hidden layers with 10 and 20 neurons in the hidden layers were analyzed. The final ANN structure (2 hidden layers with 20 neurons) was chosen as the one that gave better results in terms of R^2, MSE and RMSE when compared to the others and used comparable computational time.

Table 4 Performance associated with the developed ANNs.

	R^2 (–)	MSE ($°C^2$)	RMSE (°C)
ANNH1	0.978	0.062	0.2491
ANNH2	0.972	0.077	0.2777
ANNH3	0.972	0.079	0.2816
ANNH4	0.961	0.109	0.3307
ANNC1	0.982	0.042	0.2058
ANNC2	0.983	0.039	0.1968
ANNC3	0.976	0.058	0.2406
ANNC4	0.980	0.049	0.2218

An ANN based controller was developed in the MATLAB environment [51] and then integrated with the system models in TRNSYS [50]. In this paper the following six different artificial neural networks based strategies were proposed and investigated for controlling the GSHP-PVT system during the heating period: (1) ANN_LOGIC_H1; (2) ANN_LOGIC_H2; (3) ANN_LOGIC_H3; (4) ANN_LOGIC_H4; (5) ANN_LOGIC_H5; and (6) ANN_LOGIC_H6.

The following six different artificial neural networks based control logics were developed for the cooling period: (1) ANN_LOGIC_C1; (2) ANN_LOGIC_C2; (3) ANN_LOGIC_C3; (4) ANN_LOGIC_C4; (5) ANN_LOGIC_C5; and (6) ANN_LOGIC_C6.

Table 5 shows the system's components controlled by the ANN based controller, the condition to be satisfied in order to activate the ANN based strategy, the input variables used

Table 5 ANN-based control logics of the GSHP-PVT system.

	System's components controlled by the ANNs based controller	Condition to be satisfied for activating the ANNs based controller	Output of ANNs based controller in case of the condition specified in the previous column is satisfied[a]
ANN_LOGIC_H1	Blower fan, Main pump	The values of at least two of parameters among $T_{room,(+3h)}$, $T_{room,(+4h)}$, $T_{room,(+5h)}$, $T_{room,(+6h)}$ are greater than 21.5 °C	– Blower fan & Main pump: *OFF*
ANN_LOGIC_H2		The value of at least one of parameters among	
ANN_LOGIC_H3	Blower fan, Main pump, GSHP, GSHP pump, Tank Pump, Auxiliary heater	$T_{room,(+3h)}$, $T_{room,(+4h)}$, $T_{room,(+5h)}$, $T_{room,(+6h)}$ is greater than 21.5 °C	– Blower fan & Main pump: *OFF* – GSHP & GSHP Pump & Tank Pump: *ON if* $T_{2,HWT} \leqslant 45$ °C, *OFF if* $T_{5,HWT} \geqslant 50$ °C – Auxiliary heater: *ON if* $T_{2,HWT} \leqslant 40$°C, *OFF if* $T_{3,HWT} \geqslant 45$ °C
ANN_LOGIC_H4			– Blower fan & Main pump & GSHP & GSHP Pump & Tank Pump & Auxiliary heater: *OFF*
ANN_LOGIC_H5	Blower fan, Main pump, GSHP		– Blower fan & Main pump: *OFF* – GSHP: *operation at lower heating capacity 7.0 kW (instead of 10.5 kW)*
ANN_LOGIC_H6	GSHP		– GSHP: *operation at lower heating capacity 7.0 kW (instead of 10.5 kW)*
ANN_LOGIC_C1	Blower fan, Main pump	The values of at least two of parameters among $T_{room,(+3h)}$, $T_{room,(+4h)}$, $T_{room,(+5h)}$, $T_{room,(+6h)}$ are lower than 24.5 °C	– Blower fan & Main pump: *OFF*
ANN_LOGIC_C2		The value of at least one of parameters among	
ANN_LOGIC_C3	Blower fan, Main pump, GSHP, GSHP pump, Tank Pump	$T_{room,(+3h)}$, $T_{room,(+4h)}$, $T_{room,(+5h)}$, $T_{room,(+6h)}$ is lower than 24.5 °C	– Blower fan & Main pump: *OFF* – GSHP & GSHP Pump & Tank Pump: *ON if* $T_{5,HWT} \leqslant 15$ °C, *OFF if* $T_{9,HWT} \geqslant 12$ °C
ANN_LOGIC_C4			– Blower fan & Main pump & GSHP & GSHP Pump & Tank Pump: *OFF*
ANN_LOGIC_C5	Blower fan, Main pump, GSHP		– Blower fan & Main pump: *OFF* – GSHP: *operation at lower cooling capacity 5.3 kW (instead of 7.0 kW)*
ANN_LOGIC_C6	GSHP		– GSHP: *operation at lower cooling capacity 5.3 kW (instead of 7.0 kW)*

[a] In the case of the condition specified in the previous column is not satisfied, the system's components are operated as with the on-off control strategy.

by the ANN based controller, and the output of the ANN based approach in case when the above-mentioned condition is satisfied; the GSHP-PVT system is operated as with the on-off control strategy in the case of the conditions to activate the ANN based controller specified in Table 5 are not satisfied. As highlighted in Table 5, the two-stage GSHP can be operated at its lower heating/cooling capacity depending on the boundary conditions only under the ANN_LOGIC_H5, ANN_LOGIC_H6, ANN_LOGIC_C5 and ANN_LOGIC_C6 control logics; under the other ANN based strategies, the GSHP is always operated at its high heating/cooling capacity.

The values of the input variables $T_{room,(+3h)}$, $T_{room,(+4h)}$, $T_{room,(+5h)}$ and $T_{room,(+6h)}$ during both the heating and cooling periods are predicted by the artificial neural networks described in Table 3.

4. Methods of analysis

All ANN based control logics for both heating and cooling seasons were developed with the main goals (i) to maintain acceptable indoor conditions limiting "overheating"/"over cooling" phenomena as well as (ii) to reduce the overall primary energy consumption, operational costs and carbon dioxide equivalent emissions.

Firstly the GSHP-PVT system operation with the on-off control logic was simulated by using TRNSYS 17 under the climatic conditions of Ottawa (Canada); the simulations were performed over the whole year (the heating season is assumed to start from October 1st to May 31st, with the cooling season from the beginning of June to the end of September) with a simulation time step equal to 18 s.

Then a predictive controller was developed using artificial neural networks. Six different ANN based strategies (described in the Section 3.2) were trained and tested for both the heating and cooling periods. The performance of the GSHP-PVT system under the proposed ANN controls was simulated in TRNSYS [50] under the climatic conditions of Ottawa (Canada) using a simulation time step equal to 18 s during a single week of the heating period (May 1st–May 7th) as well as a single week of the cooling period (July 1st–July 7th). The study was limited to the two above-mentioned weeks in order to (i) operate with a reasonable computation time as well as (ii) focus on the periods where the "overheating"/"over cooling" phenomena are relevant when compared to the rest of the year.

The on-off strategy and the ANN based approaches were first compared in terms of capability in maintaining the desired comfort conditions.

In addition, the comparison was performed from an energy point of view by means of the following indicator PED (Primary Energy Difference):

$$PED = \left(E_p^{on-off} - E_p^{ANN}\right)/E_p^{on-off} \quad (4)$$

where E_p^{on-off} and E_p^{ANN} represent the total primary energy consumption of the whole GSHP-PVT system with on-off control logic and ANNs based approach, respectively, due to the operation of all the components of the GSHP-PVT system (main pump, blower fan, GSHP, GSHP pump, tank pump, PVT pump, solar preheat pump and natural gas auxiliary heater). The primary energy factor is assumed as 2.6 for the electricity (feed and from the grid) and 1.1 for natural gas (to consider 10% of overhead for delivery to the site). The primary energy factor for the electricity is determined by post-processing data reported in [64,65], while the primary energy factor for the natural gas is obtained according to the values suggested in [66]. In the primary energy calculation the higher heating value of natural gas is considered equal to 37,074 kJ/m^3 with a density of 0.668 kg/m^3.

A positive value of the PED indicates that the ANN approach is characterized by a reduced primary energy consumption when compared to the traditional logic.

The economic comparison between the on-off control logic and the ANN based strategies was carried out in terms of the operational costs as follows:

$$\Delta CO = \left(CO^{on-off} - CO^{ANN}\right)/CO^{on-off} \quad (5)$$

where CO^{on-off} and CO^{ANN} represent the annual operational costs of the GSHP-PVT system with on-off control logic and ANNs based approach, respectively. In the Ottawa area, there are two electricity billing structures, "tiered" and "time of use (TOU)". The tiered electricity price is 0.14426 CAD/kW h for the first 750 kW h and 0.15846 CAD/kW h for additional usage. The TOU price periods consist of off-peak, mid-peak and on-peak which are different between the winter and summer: in particular, the TOU electricity price is 0.12646 CAD/kW h off-peak, 0.16246 CAD/kW h mid-peak and 0.18146 CAD/kW h on-peak. The application of the TOU prices is to encourage users to shift from on-peak to off-peak periods to manage electricity costs, reduce strain on the electricity system and help the environment. In this paper the annual electricity costs were calculated based on TOU billing structure taking into account that the majority of customers are billed by TOU; the electricity selling rate was assumed at 75% of the purchase price. The natural gas price was tiered and ranged from 0.216 to 0.244 CAD/m^3 depending on the monthly volume usage.

The ANN based approach was compared to a conventional on-off strategy also from an environmental point of view. A simplified approach was adopted in this paper by considering the carbon dioxide equivalent emissions using an energy output-based emission factor approach [67]. In particular, the environmental comparison was calculated by using the following indicator:

$$\Delta CO_2 = \left(CO_2^{on-off} - CO_2^{ANN}\right)/CO_2^{on-off} \quad (6)$$

The parameters CO_2^{on-off} and CO_2^{ANN} represent the carbon dioxide equivalent emissions of the GSHP-PVT system with the on-off logic and the ANNs based approach, respectively. In this study, the CO_2 emission factors for natural gas and electricity (feed and from the grid) were assumed equal to 235 $gCO_2/kW\,h_p$ and 590 $gCO_2/kW\,h_{el}$, respectively, according to the values specified in [68]. A positive value of ΔCO_2 indicates that the proposed ANN based strategies allow to reduce the equivalent CO_2 emissions in comparison with the conventional control.

5. Comfort results and discussion

The relevance of both "overheating" and "overcooling" associated with the GSHP-PVT system operation with the on-off

control logic was first analyzed by calculating the following two parameters ΔT_{OH} and ΔT_{OC}:

$$\Delta T_{OH} = T_{room} - 21.5\ ^{\circ}C \quad (7)$$

$$\Delta T_{OC} = 24.5\ ^{\circ}C - T_{room} \quad (8)$$

ΔT_{OH} indicates the relevance of "overheating" being the difference between the actual room temperature obtained from the simulations and 21.5 °C (upper limit of the desirable thermal comfort zone during the heating period), while ΔT_{OC} describes the relevance of "overcooling" being the difference between 24.5 °C (lower limit of the desirable thermal comfort zone during the cooling period) and the simulated actual room temperature.

Fig. 2a and b report the positive values of the parameters ΔT_{OH} and ΔT_{OC}, respectively, as a function of the simulation time obtained by simulating the GSHP-PVT system operating under the on-off control logic. Fig. 2a highlights that ΔT_{OH} is positive during a period of 960.9 h (corresponding to around 16.5% of the whole heating period duration); the maximum and the average of the positive values of ΔT_{OH} result equal to 9.30 °C and 2.83 °C, respectively. Fig. 2b shows that the portion of the cooling period characterized by a simulated room temperature lower than 24.5 °C ($\Delta T_{OC} > 0$) has a duration of 1161.9 h (corresponding to 39.7% of the whole cooling period duration); the maximum and average of the positive values of ΔT_{OC} are equal to 9.26 °C and 2.21 °C, respectively.

Fig. 2a highlights that, in case the on-off control strategy is used, the overheating phenomena are relevant mainly during both April and May (when the contribution of solar gains is large), while they are almost negligible during the remaining part of the heating season; the overcooling phenomena (Fig. 2b) are not negligible during the whole duration of the cooling season with the largest peaks observed mainly during September.

The two figures point out that both the "overheating" and "overcooling" are relevant and, therefore, a controller having the ability to forecast the building thermal behavior up to a certain time horizon can significantly reduce the primary energy, operational costs and CO_2 equivalent emissions required for maintaining the indoor conditions within the comfort zone.

For example, Fig. 3a and b show the trend of the ambient temperature, the solar irradiance over a horizontal surface, the internal gains (generated by persons, light bulbs and house appliances) as well as the room temperature with the on-off control as a function of the time during, respectively, a typical day of the week from May 1st to May 7th and a typical day of the week of July 1st–July 7th. The indoor temperature in the case of operation under the control logic ANN_LOGIC_H5

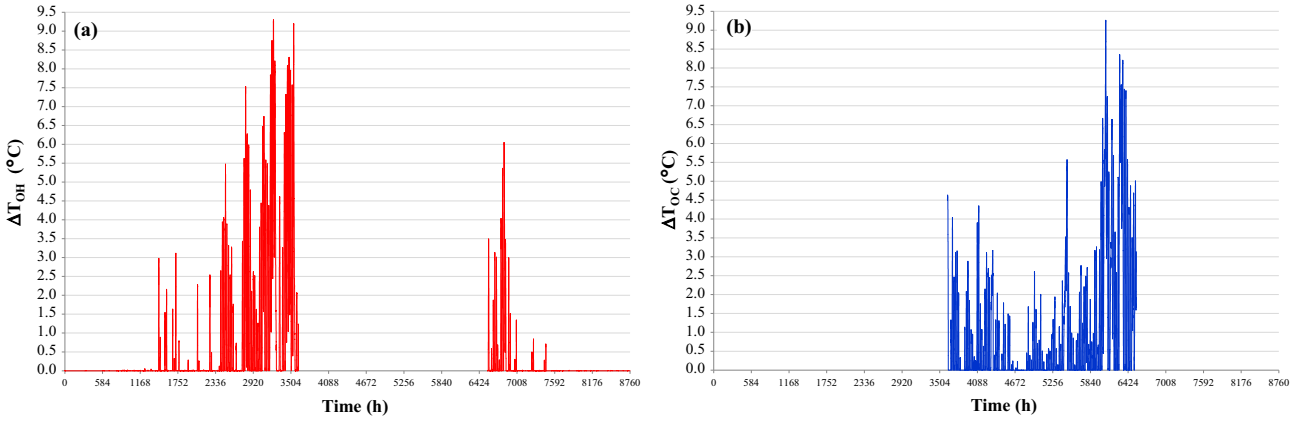

Figure 2 "Overheating" period (a) and "overcooling" period (b) with on-off control.

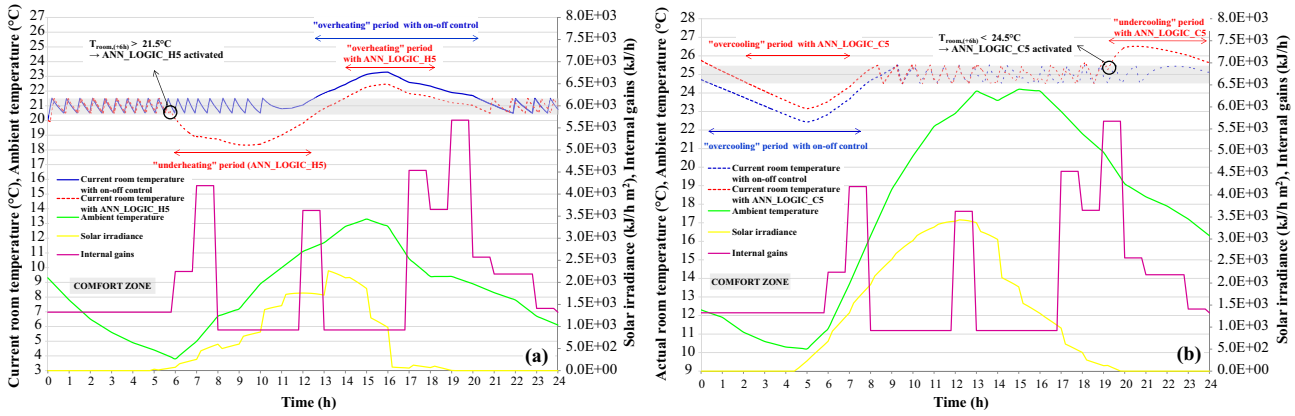

Figure 3 Typical daily operation with on-off control and ANNs based approach during (a) the week from May 1st to May 7th and (b) the week from July 1st to July 7th.

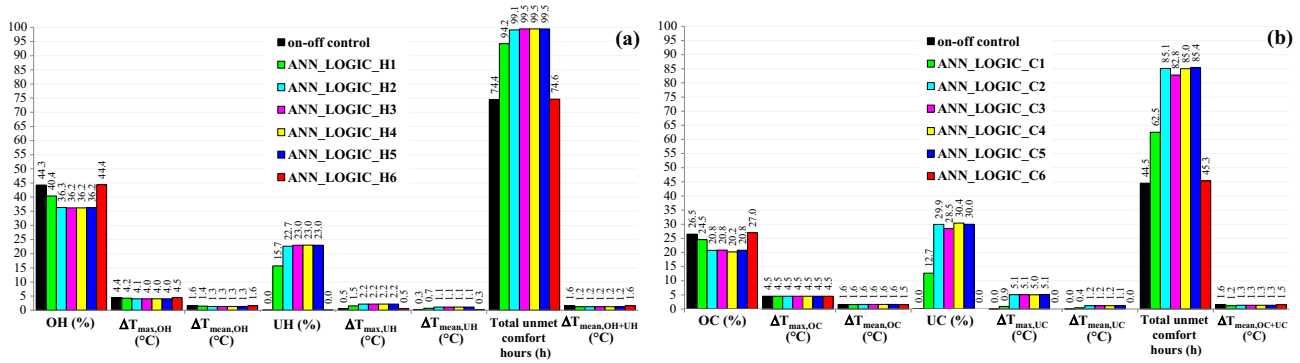

Figure 4 "Overheating" and "underheating" during the week from May 1st to May 7th (a), "overcooling" and "undercooling" during the week from July 1st to July 7th (b).

(assumed as an example of the ANN based strategies developed for the heating period) is also reported in Fig. 3a, while Fig. 3b highlights the trend of the indoor temperature with the strategy ANN_LOGIC_C5 (assumed as an example of the ANNs based strategies for the cooling period). The comfort zone (indoor temperature from 20.5 °C and 21.5 °C during the heating period and from 24.5 °C and 25.5 °C during the cooling period) as well as the activation instant of the ANNs based control logics are specified in both figures. Both the "overheating" period (period with the actual room temperature higher than 21.5 °C) and the "underheating" period (period with actual room temperature lower than 20.5 °C) are also indicated in Fig. 3a, while Fig. 3b shows both the "overcooling" period (period with actual room temperature lower than 24.5 °C) and the "undercooling" period (period with the actual room temperature larger than 25.5 °C).

Fig. 3a highlights that, even if the heating system is switched-off, the room temperature with on-off control is higher than 21.5 °C ("overheating") from around noon up to around 8 p.m. due to the increase in ambient temperature, solar irradiance and internal gains. The ANN_LOGIC_H5 strategy stops both main pump and blower fan (and operates the GSHP at lower heating capacity) at around 6 a.m. thanks to the fact that the ANN control "knows" that the room temperature will be higher than 21.5 °C after six hours of operation. This causes the room temperature to be slightly out of the thermal comfort zone becoming lower than 20.5 °C ("underheating"), but at the same time it significantly reduces both the duration and intensity of the "overheating" period.

Similarly, Fig. 3b indicates that, even if the cooling system is switched-off, the room temperature with on-off control is lower than 24.5 °C ("overcooling") from around midnight up to around 8 a.m. due to low values of ambient temperature, solar irradiance and internal gains. If compared to the on-off control, the ANN_LOGIC_C5 logic can strongly minimize the significance of the "overcooling" phenomena; however, the room temperature becomes slightly higher than the upper limit of the desirable thermal comfort zone ("undercooling") during a limited time due the activation of the ANN based approach.

The capability of the ANN based strategies in controlling the indoor conditions is detailed in the Fig. 4a and b with reference to the heating and cooling periods, respectively.

In particular, Fig. 4a reports the following parameters related to the operation of both the on-off control and the six ANNs based heating control strategies (H1–H6):

- the time percentage OH during which actual room temperature is higher than 21.5 °C (i.e. the duration of the "overheating" period);
- the maximum difference $\Delta T_{max,OH}$ between the actual room temperature and 21.5 °C;
- the average difference $\Delta T_{mean,OH}$ between the actual room temperature and 21.5 °C;
- the time percentage UH during which the actual room temperature is lower than 20.5 °C (i.e. the duration of the "underheating" period);
- the maximum difference $\Delta T_{max,UH}$ between 20.5 °C and the actual room temperature;
- the average difference $\Delta T_{max,UH}$ between 20.5 °C and the actual room temperature;
- the total number of unmet comfort hours (due to both overheating and underheating phenomena);
- the average temperature difference with the comfort zone $\Delta T_{mean,OH+UH}$ (this parameter is calculated as the arithmetic mean of the following positive differences only (T_{room} – 21.5 °C) and (20.5 °C – T_{room})).

Fig. 4b presents the indoor conditions associated with the operation of both on-off control and six ANNs based cooling control strategies (C1–C6). The following parameters are reported:

- the time percentage OC during which the actual room temperature is lower than 24.5 °C (i.e. the duration of the "overcooling" period);
- the maximum difference $\Delta T_{max,OC}$ between 24.5 °C and the actual room temperature;
- the average difference $\Delta T_{mean,OC}$ between 24.5 °C and the actual room temperature;
- the time percentage UC during which the actual room temperature is larger than 25.5 °C (i.e. the duration of the "undercooling" period);
- the maximum difference $\Delta T_{max,UC}$ between the actual room temperature and 25.5 °C;
- average difference $\Delta T_{mean,UC}$ between the actual room temperature and 25.5 °C;
- the total number of unmet comfort hours (due to both overcooling and undercooling phenomena);
- the average temperature difference with the comfort zone $\Delta T_{mean,OC+UC}$ (this parameter is calculated as the arithmetic mean of the following positive differences only (T_{room} – 25.5 °C) and (24.5 °C – T_{room})).

Fig. 4a indicates that the on-off control is unable to guarantee the specifications of the comfort zone (due to overheating or underheating phenomena) during a period of around 74.4 h, with an average temperature difference in comparison with the comfort ($\Delta T_{mean,OH+UH}$) equal to 1.6 °C. This figure also shows that, when compared to the on-off control, the ANN based logics (except the ANN_LOGIC_H6 strategy):

- allow to significantly limit the duration of the "overheating" period (the values of OH decrease from 44.3% down to 36.2%);
- allow to reduce the intensity of the "overheating" period with a reduction in the values of both $\Delta T_{max,OH}$ (from 4.4 °C down to 4.0 °C) and $\Delta T_{mean,OH}$ (from 1.6 °C down to 1.3 °C);
- cause an enhancement of the duration of the "underheating" period (the values of UH increase up to 23.0%) as well as slightly increase the intensity of the "underheating" with larger values of both $\Delta T_{max,UH}$ (up to 2.2 °C) and $\Delta T_{mean,UH}$ (up to 1.1 °C). This is mainly due to the earlier shutdown of system's components controlled by the ANN based strategies;
- increase the total number of hours where both overheating or underheating occur (with a maximum percentage increment equal to around 25%);
- alleviate the average temperature gap with the comfort zone (with a maximum percentage reduction of about 22%).

The simulation results do not highlight significant differences between the ANN_LOGIC_H6 strategy and the on-off control in terms of ability to maintain the desired indoor temperature. In addition, it can be noted that the ANN_LOGIC_H1 logic allows to slightly reduce the total number of unmet comfort hours in comparison with the ANN_LOGIC_H2, ANN_LOGIC_H3, ANN_LOGIC_H4, and ANN_LOGIC_H5 strategies.

Similarly, Fig. 4b highlights that the simple on-off strategy does not allow to fully meet the desired indoor conditions (due to both overcooling and undercooling) during a period of around 44.5 h (less relevant if compared to the week May 1st–May 7th), characterized by an average temperature difference with the comfort zone ($\Delta T_{mean,OC+UC}$) equal to 1.6 °C (same value for the week May 1st–May 7th). This figure also demonstrates that, in comparison with the traditional control, the logics based on ANNs (except the ANN_LOGIC_C6 strategy):

- allow to significantly limit the duration of the "overcooling" period (the values of OC decrease from 26.5% down to 20.2%);
- do not affect the intensity of the "overcooling" period (no significant changes of both $\Delta T_{max,OC}$ and $\Delta T_{mean,OC}$ can be obtained);
- cause an increased duration of the "undercooling" period (the values of UC increase up to 30.4%) and slightly increase the intensity of the "undercooling" with larger values of both $\Delta T_{max,UC}$ (up to 5.1 °C) and $\Delta T_{mean,UC}$ (up to 1.2 °C). This is mainly due to the earlier stop of system's components based on the room temperature prediction performed by the ANN controllers;
- increase the total number of hours characterized by overcooling or underheating phenomena (with a maximum percentage increment equal to around 48%);
- alleviate the average temperature difference with the comfort zone (with a maximum percentage reduction of about 14%).

In comparison with the on-off control, the ANN_LOGIC_C6 strategy provides similar results in terms of both the number of unmet comfort hours and values of $\Delta T_{mean,OC+UC}$. The simulation results also highlighted that the ANN_LOGIC_C1 logic allows to obtain better results in terms of ability to maintain the indoor specifications when compared to the ANN_LOGIC_C2, ANN_LOGIC_C3, ANN_LOGIC_C4, and ANN_LOGIC_C5 strategies.

6. Energy results and discussion

The simulation results obtained with the ANNs based approaches were compared with those associated with the traditional on-off logic also from the primary energy consumption.

Fig. 5 indicates the weekly primary energy consumption associated with each single components of the GSHP-PVT system with the on-off control. It can be noted that the GSHP is in charge of the most part (more than 65%) of the overall primary energy demand, while the primary energy consumptions of the boiler, PVT pump, and solar preheat pump are almost negligible.

Fig. 6a shows the total primary energy difference (calculated according to the Eq. (4)) associated with the six ANN based heating control strategies (ANN_LOGIC_H1-H6) in comparison with the on-off logic with respect to the operation during the week of May 1st–May 7th. Fig. 6b highlights the values of PED (calculated according to the Eq. (4)) for the six ANN based cooling control strategies (ANN_LOGIC_C1-C6) in comparison with the on-off logic for the week of July 1st–July 7th.

The results reported in Fig. 6a and b can be summarized as follows:

- all ANN based control logics investigated in this work allow to reduce the primary energy consumption in comparison with the on-off strategy (this is mainly due to the fact that the total operation time of the system's components controlled by the ANN based strategies is reduced);
- the overall primary energy reductions achievable during the week of July 1st–July 7th are larger than those associated with the week of May 1st–May 7th;
- during the week of May 1st–May 7th, the ANN_LOGIC_H1, ANN_LOGIC_H2, ANN_LOGIC_H3 and ANN_LOGIC_H4 logics provide similar results in terms of PED (around 11%);
- during the week of July 1st–July 7th, the ANN_LOGIC_C5 strategy achieves the best primary energy reduction (36%);
- the system performance under the ANN_LOGIC_H6 and ANN_LOGIC_C6 strategies highlights that the system does not greatly benefit in the case when only the staged GSHP operation is considered during the shoulder heating/cooling periods.

Please cite this article in press as: E. Entchev et al., Energy, economic and environmental performance simulation of a hybrid renewable microgeneration system with neural network predictive control, Alexandria Eng. J. (2016), http://dx.doi.org/10.1016/j.aej.2016.09.001

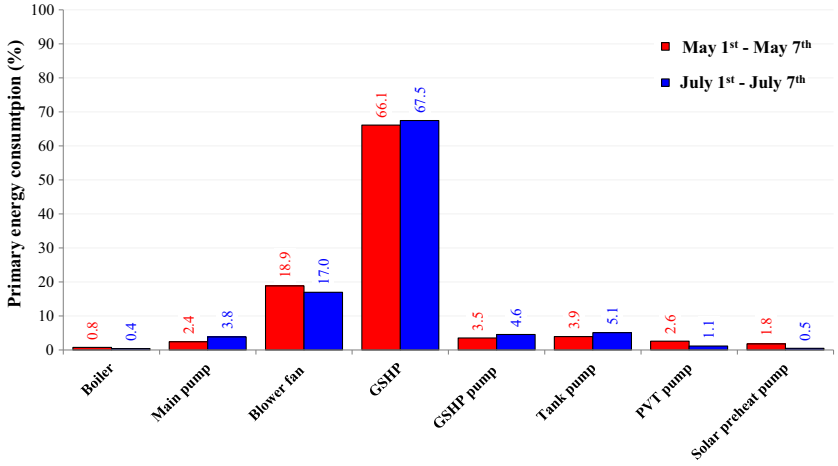

Figure 5 Percentage of weekly primary energy consumption associated with the single components of the GSHP-PVT scheme with the on-off control.

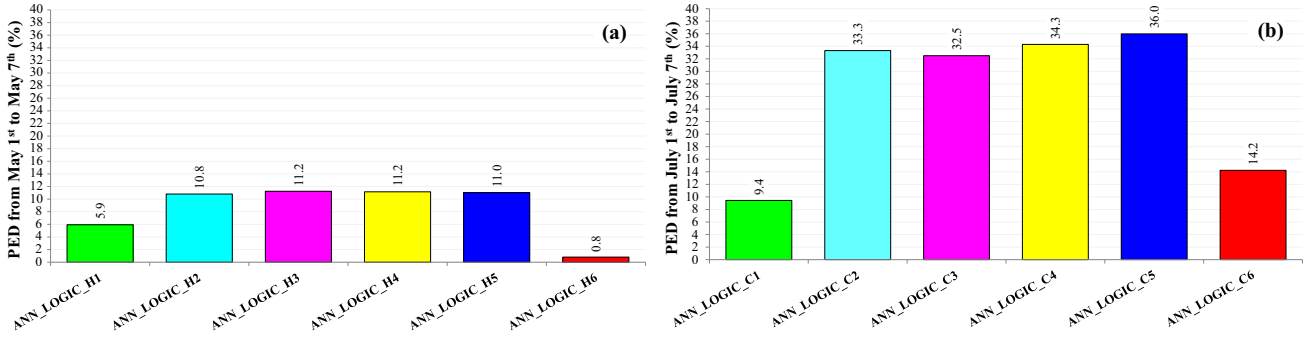

Figure 6 Total primary energy difference PED during (a) the week from May 1st to May 7th and (b) during the week from July 1st to July 7th.

7. Economic results and discussion

In addition to the energy analysis, the on-off control logic and the ANN based strategies were also compared from an economic point of view in terms of operational costs.

Fig. 7a shows the values of ΔCO (calculated according to the Eq. (5)) for the six ANNs based heating control strategies (H1–H6) in comparison with the on-off logic. Fig. 7b indicates the values of ΔCO (calculated according to the Eq. (5)) associated with six ANNs based control strategies (C1-C6) for the cooling period in comparison with the on-off logic.

Fig. 7a and b highlight that:

– the system with ANNs based control logics has lower operational costs when compared to the one with on-off control (this is mainly due to the fact that the total operation time of the system components managed by the ANN based controllers is reduced);

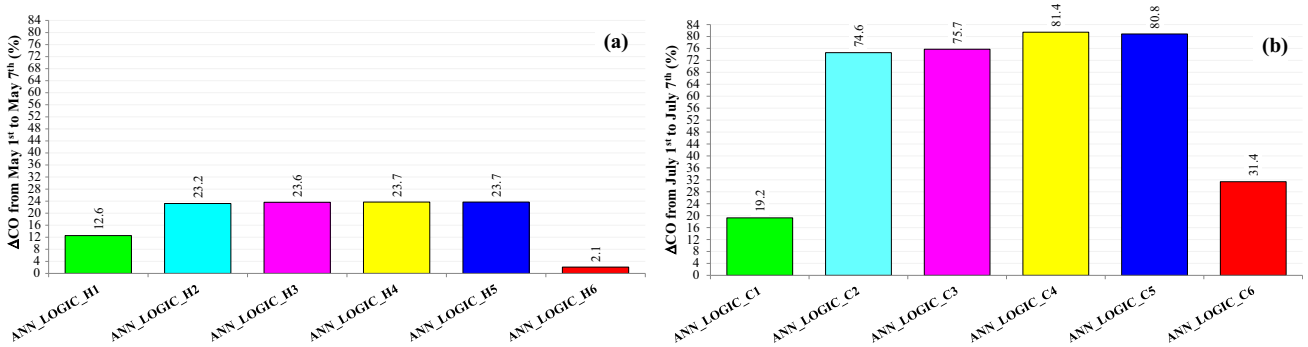

Figure 7 Total operational cost saving ΔCO associated with the ANNs based control strategies during (a) the week from May 1st to May 7th and (b) during the week from July 1st to July 7th.

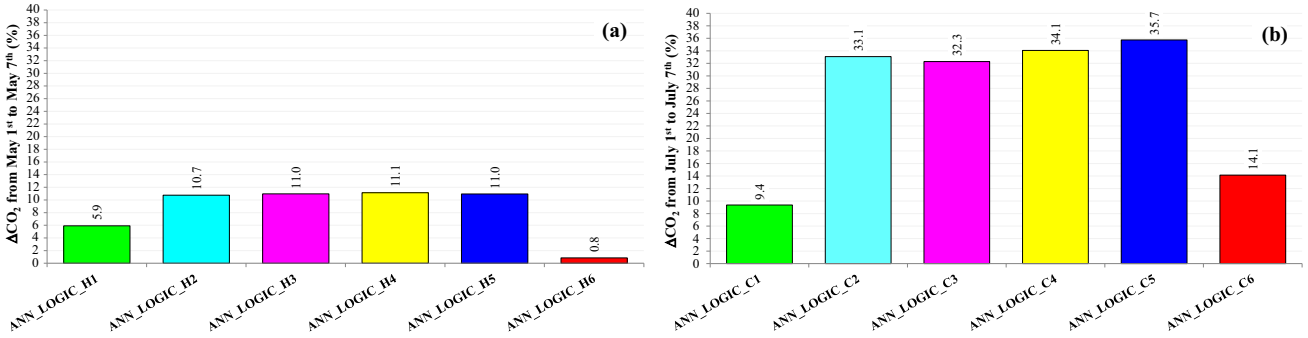

Figure 8 Reduction in carbon dioxide equivalent emissions ΔCO_2 associated with the ANNs based control strategies during (a) the week from May 1st to May 7th and (b) during the week from July 1st to July 7th.

- the operational cost reductions achievable during the week of July 1st–July 7th are greater than those associated with the week from May 1st to May 7th;
- during the week of May 1st–May 7th, the ANNs based control logics ANN_LOGIC_H1, ANN_LOGIC_H2, ANN_LOGIC_H3, and ANN_LOGIC_H4 provide similar results (the operational cost is reduced by around 24%);
- during the week from July 1st to July 7th, the largest operational cost reduction (around 81%) is obtained in the case of the ANNs based control logics ANN_LOGIC_C4 and ANN_LOGIC_C5 are used;
- the sole staged GSHP operation (ANN_LOGIC_H6 and ANN_LOGIC_C6 strategies) does not really benefited the economic performance of the GSHP/PVT system.

With respect to the capital costs, it is still very challenging to achieve their estimation with a good accuracy for systems with ground source heat pumps and PVT panels due to their immature market share. Nevertheless, it is estimated that the initial cost increment for the studied GSHP-PVT system is likely exceeding the cumulative cost savings over their life span due to high cost associated with the ground heat exchanger drilling and solar collectors array. This means that the additional investment could not be fully returned within the life span of the system. Although it seems that the hybrid GSHP-PVT microgeneration system is not very cost-effective at current market prices, it would be economically feasible if economic incentives in conjunction with price reductions on equipment/installation resulting from economy of scale and market expansion are considered.

8. Environmental results and discussion

In this section the results of the environmental analysis were reported and discussed.

Fig. 8a shows the values of ΔCO_2 (calculated according to the Eq. (6)) for the six ANNs based heating control strategies (H1–H6) in comparison with the on-off logic. Fig. 7b indicates the values of ΔCO_2 (calculated according to the Eq. (6)) associated with six ANNs based control logics for the cooling period (C1–C6) in comparison with the conventional approach.

Fig. 8a and b indicates that the results of the environmental analysis are quite similar to those of the energy analysis:

- all ANN based control strategies investigated in this paper reduce the carbon dioxide equivalent emissions in comparison with the on-off strategy;
- the overall reduction of the CO_2 equivalent emissions during the week of July 1st–July 7th are larger than those associated with the week of May 1st–May 7th;
- during the week of May 1st–May 7th, the ANN_LOGIC_H1, ANN_LOGIC_H2, ANN_LOGIC_H3 and ANN_LOGIC_H4 logics provide similar results in terms of ΔCO_2 (around 11%);
- during the week of July 1st–July 7th, the ANN_LOGIC_C5 strategy achieves the largest reduction in the carbon dioxide equivalent emissions (around 34%);
- the simulation data under the ANN_LOGIC_H6 and ANN_LOGIC_C6 strategies highlight that the system does not greatly benefit in the case when only the staged GSHP operation is considered during the shoulder heating/cooling periods.

9. Conclusions

In this study the potential energy and cost savings of a GSHP-PVT system serving a detached residential Canadian house under different control strategies based on Artificial Neural Networks and conventional on-off control were investigated.

The simulations performed in TRNSYS dynamic simulation environment comparing both strategies in terms of ability in controlling the indoor conditions highlighted that the proposed control logics using artificial neural networks:

- are able to reduce the temperature swings outside the comfort zone (up to around 22% during the week of May 1st–May 7th and 14% during the week of July 1st–July 7th);
- generally cause an increase in unmet comfort hours due to the enhancement of the "underheating" during the period from May 1st to May 7th (with a percentage increment up to around 25%) as well as the "undercooling" during the period from July 1st to July 7th (up to a maximum of around 48%);

From an energy point of view, the simulation data highlighted that the ANN based strategies lead to lower primary energy consumption with a reduction up to 11% during the

week of May 1st–May 7th and 36% during the week of July 1st–July 7th. Similar results were obtained from the environmental analysis in terms of carbon dioxide equivalent emissions.

The results of the economic comparison with the traditional on-off control highlighted that:

- the operating costs can be significantly lowered by using the proposed ANN control logics up to 24% during the week of May 1st–May 7th and 81% during the week of July 1st–July 7th;
- for all ANN based control logics the operational cost reduction is more relevant if compared to the primary energy/CO_2 emissions reduction thanks to the fact that the ANN strategies not only reduce the operational costs for the electric energy purchased from the grid, but they also enhance the revenues associated with the exported electricity.

Additional control strategies should be investigated in the future, such as (i) linking the operation of the fan blower to the temperature of the circulating water by the main pump and/or (ii) using modulating three-way valves/pumps, in order to explore in more detail the potential advantages and possible drawbacks of the ANN approach applied to complex hybrid heating/cooling systems.

Acknowledgments

This work was supported by the International Cooperation of Korea Institute of Energy Technology Evaluation and Planning (KETEP) grant funded by the Korea Government Ministry of Knowledge Economy (No. 20118520010010). Financial support from both Canadian and Republic of Korea governments is gratefully acknowledged. The authors also wish to acknowledge the collaboration and contributions of Dr. EJ. Lee and his team from Korea Institute of Energy Research (KIER), Dr. Soolyeon CHO from School of Architecture, North Carolina State University, Raleigh, NC, USA, and IBC Technologies Inc., Vancouver, Canada, for providing the boiler performance specifications.

References

[1] BP Statistical Review of World Energy, June 2013, <http://www.bp.com/content/dam/bp-country/fr_fr/Documents/Rapportsetpublications/statistical_review_of_world_energy_2013.pdf> (last accessed on January 2016).
[2] Directive 2004/8/EC of the European Parliament and of the Council of the 11 February 2004 on the promotion of cogeneration based on the useful heat demand in the internal energy market and amending Directive 92/42/EEC. Official Journal of the European Union, 2004.
[3] M.M. Maghanki, B. Ghobadian, G. Najafi, R.J. Galogah, Micro combined heat and power (MCHP) technologies and applications, Renew. Sustain. Energy Rev. 28 (2013) 510–524.
[4] S. Evangelisti, P. Lettieri, R. Clift, D. Borello, Distributed generation by energy from waste technology: a life cycle perspective, Process Saf. Environ. Prot. 93 (2015) 161–172.
[5] G. Angrisani, C. Roselli, M. Sasso, Distributed microtrigeneration systems, Prog. Energy Combust. Sci. 38 (2012) 502–521.
[6] D. Sonar, S.L. Soni, D. Sharma, Micro-trigeneration for energy sustainability: Technologies, tools and trends, Appl. Therm. Eng. 71 (2014) 790–796.
[7] H.I. Onovwiona, V.I. Ugursal, Residential cogeneration systems: review of current technology, Renew. Sustain. Energy Rev. 10 (2006) 389–431.
[8] D.W. Wu, R.Z. Wang, Combined cooling, heating and power: a review, Prog. Energy Combust. Sci. 32 (2006) 459–495.
[9] IEA/ECBCS Annex 42 - The Simulation of Building-Integrated Fuel Cell and Other Cogeneration Systems (COGEN-SIM), <http://www.ecbcs.org/annexes/annex42.htm> (last accessed on January 2016).
[10] IEA/ECBCS Annex 54 - Integration of Micro-Generation and Related Energy Technologies in Buildings, <http://iea-annex54.org/index.html> (last accessed on January 2016).
[11] C. Ferrari, F. Melino, M. Pinelli, P.R. Spina, M. Venturini, Overview and status of thermophotovoltaic systems, Energy Proc. 45 (2014) 160–169.
[12] A. Kumar, P. Baredar, U. Qureshi, Historical and recent development of photovoltaic thermal (PVT) technologies, Renew. Sustain. Energy Rev. 42 (2015) 1428–1436.
[13] T.T. Chow, A review on photovoltaic/thermal hybrid solar technology, Appl. Energy 87 (2010) 365–379.
[14] P. Bayer, D. Saner, S. Bolay, L. Rybach, P. Blum, Greenhouse gas emission savings of ground source heat pump systems in Europe: a review, Renew. Sustain. Energy Rev. 16 (2012) 1256–1267.
[15] S.J. Self, B.V. Reddy, M.A. Rosen, Geothermal heat pump systems: status review and comparison with other heating options, Appl. Energy 101 (2013) 341–348.
[16] A.M. Omer, Ground-source heat pumps systems and applications, Renew. Sustain. Energy Rev. 12 (2008) 344–371.
[17] I. Sarbu, C. Sebarchievici, General review of ground-source heat pump systems for heating and cooling of buildings, Energy Build. 70 (2014) 441–454.
[18] S. Sibilio, M. Sasso, R. Possidente, C. Roselli, Assessment of micro-cogeneration potential for domestic trigeneration, Int. J. Environ. Technol. Manage. 7 (2007) 147–164.
[19] D. Sonar, S.L. Soni, D. Sharma, Micro-trigeneration for energy sustainability: technologies, tools and trends, Appl. Therm. Eng. 71 (2014) 790–796.
[20] J. Gusdorf, M. Douglas, M. Swinton, F. Szadkowski, M. Manning, Testing a residential system including combined heat and power and ground heat source heat pumps at the Canadian Centre for Housing Technology, 1st International Conference on Microgeneration and Related Technologies, Ottawa, April 2008.
[21] T. Guo, H.X. Wang, S.J. Zhang, Selection of working fluids for a novel low temperature geothermally-powered ORC based cogeneration system, Energy Convers. Manage. 52 (2011) 2384–2391.
[22] H. Ribberink, K. Lombardi, L. Yang, E. Entchev, Hybrid renewable microgeneration energy system for power and thermal generation with reduced emissions, in: 2nd International Conference on Microgeneration and Related Technologies. Glasgow, April 2011.
[23] S. Obara, S. Watanabe, B. Rengarajan, Operation method study based on the energy balance of an independent microgrid using solar-powered water electrolyzer and an electric heat pump, Energy 36 (2011) 5200–5213.
[24] B. Twomey, P.A. Jacobs, H. Gurgenci, Dynamic performance estimation of small-scale solar cogeneration with an organic Rankine cycle using a scroll expander, Appl. Therm. Eng. 51 (2013) 1307–1316.
[25] F. Calise, Design of a hybrid polygeneration system with solar collectors and a solid oxide fuel cell: dynamic simulation and economic assessment, Int. J. Hydrogen Energy 36 (2011) 6128–6150.

[26] F. Calise, M. Dentice d'Accadia, L. Vanoli, Design and dynamic simulation of a novel solar trigeneration system based on hybrid photovoltaic/thermal collectors (PVT), Energy Convers. Manage. 60 (2012) 214–225.
[27] F. Calise, M. Dentice d'Accadia, A. Palombo, L. Vanoli, Dynamic simulation of a novel high-temperature solar trigeneration system based on concentrating photovoltaic/thermal collectors, Energy 61 (2013) 72–86.
[28] F. Calise, G. Ferruzzi, L. Vanoli, Transient simulation of polygeneration systems based on PEM fuel cells and solar heating and cooling technologies, Energy 41 (2012) 18–30.
[29] D. Tempesti, G. Manfrida, D. Fiaschi, Thermodynamic analysis of two micro CHP systems operating with geothermal and solar energy, Appl. Energy 97 (2012) 609–617.
[30] D. Tempesti, D. Fiaschi, Thermo-economic assessment of a micro CHP system fuelled by geothermal and solar energy, Energy 58 (2013) 45–51.
[31] E. Entchev, L. Yang, M. Ghorab, E.J. Lee, Simulation of hybrid renewable microgeneration systems in load sharing applications, Energy 50 (2013) 252–261.
[32] L. Yang, E. Entchev, M. Ghorab, E.J. Lee, E.C. Kang, Energy and cost analyses of a hybrid renewable microgeneration system serving multiple residential and small office buildings, Appl. Therm. Eng. 65 (2014) 477–486.
[33] E. Entchev, L. Yang, M. Ghorab, E.J. Lee, Performance analysis of a hybrid renewable microgeneration system in load sharing applications, Appl. Therm. Eng. 71 (2014) 697–704.
[34] M. Canelli, E. Entchev, M. Sasso, L. Yang, M. Ghorab, Dynamic simulations of hybrid energy systems in load sharing application, Appl. Therm. Eng. 78 (2015) 315–325.
[35] M. Mohanraj, S. Jayaraj, C. Muraleedharan, Applications of artificial neural networks for refrigeration, air-conditioning and heat pump systems - a review, Renew. Sustain. Energy Rev. 16 (2012) 1340–1358.
[36] H. Huang, L. Chen, E. Hu, A new model predictive control scheme for energy and cost savings in commercial buildings: an airport terminal building case study, Build. Environ. 89 (2015) 203–216.
[37] A.A. Argiriou, I. Bellas-Velidis, M. Kummert, P. André, A neural network controller for hydronic heating systems of solar buildings, Neural Networks 17 (2004) 427–440.
[38] S.M.T. Sameni, M. Gaterell, A. Montazami, A. Ahmed, Overheating investigation in UK social housing flats built to the Passivhaus standard, Build. Environ. 92 (2015) 222–235.
[39] A. Mavrogianni, M. Davies, J. Taylor, Z. Chalabi, P. Biddulph, E. Oikonomou, P. Das, B. Jones, The impact of occupancy patterns, occupant-controlled ventilation and shading on indoor overheating risk in domestic environments, Build. Environ. 78 (2014) 183–198.
[40] Y.V. Parkale, Comparison of ANN Controller and PID Controller for Industrial Water Bath Temperature Control System using MATLAB Environment, Int. J. Comput. Appl. 53 (2012) 1–6.
[41] A. Muhammad, On replacing PID controller with ANN controller for DC motor position control, Int. J. Res. Stud. Comput. 2 (2013) 21–29.
[42] S.A. Kalogirou, Neural network modeling of energy systems, Encyclopedia Energy (2004) 291–299.
[43] A. Kanarchos, K. Geramanis, Multivariable control of single zone hydronic heating system with neural networks, Energy Convers. Manage. 39 (1998) 1317–1336.
[44] A.A. Argiriou, I. Bellas-Velidis, C.A. Balaras, Development of a neural network heating controller for solar buildings, Neural Networks 13 (2000) 811–820.
[45] A.E. Ruano, E.M. Crispim, E.Z.E. Conceição, M.M.J.R. Lúcio, Prediction of building's temperature using neural networks models, Energy Build. 38 (2006) 682–694.
[46] B. Thomas, M. Soleimani-Mohseni, Artificial neural network models for indoor temperature prediction: investigations in two buildings, Neural Comput. Appl. 16 (2007) 81–89.
[47] Q. Li, Q. Meng, J. Cai, H. Yoshino, A. Mochida, Predicting hourly cooling load in the building: a comparison of support vector machine and different artificial neural networks, Energy Convers. Manage. 50 (2009) 90–96.
[48] P.M. Ferreira, A.E. Ruano, S. Silva, E.Z.E. Conceição, Neural networks based predictive control for thermal comfort and energy savings in public buildings, Energy Build. 55 (2012) 238–251.
[49] T. Salque, P. Riederer, D. Marchio, Development of a Neural Network-based Building Model and Application to Geothermal Heat Pumps Predictive Control, SIMUL 2012: The Fourth International Conference on Advances in System Simulation. November 18–23, 2012, Lisbon, Portugal.
[50] Solar Energy Laboratory, TRNSYS, Transient System Simulation Tool, version 17, Tech. rep., University of Wisconsin, Madison, USA, 2004. <http://www.trnsys.com/> (last accessed on January 2016).
[51] MathWorks. <http://www.mathworks.com/products/matlab/index.html?s_tid=gn_loc_drop> (last accessed on January 2016).
[52] Drake Landing Solar Community, <http://www.dlsc.ca/> (last accessed on August 2016).
[53] ENERTECH, WT series water-to-water heat pumps & hydronic air handlers/ "A" Coils: Engineering Data and Installation Manual, 2011, <www.enertechgeo.com> (last accessed on January 2016).
[54] ENERTECH, Engineering Data and Installation Manual, WT MODELS WATER-TO-WATER HEAT PUMPS & HYDRONIC AIR HANDLERS, <http://residential.geocomfort.com/products/literature/20D082-08NN.pdf> (last accessed on August 2016).
[55] ASHRAE standard 90.1, Energy Standard for Buildings except Low-Rise Residential Buildings, 2007.
[56] G. Angrisani, M. Canelli, C. Roselli, M. Sasso, Calibration and validation of a thermal energy storage model: influence on simulation results, Appl. Therm. Eng. 67 (2014) 190–200.
[57] VDI 4640, Thermal use of the Underground e Ground Source Heat Pump Systems, 2001.
[58] I. Katic, Measurement Report - Test of PV/T Module "PVtwin", Danish Technological Institute, 2006, <http://www.iea-shc.org/data/sites/1/publications/DC4-1_Measurement_Report_Test_of_PVT_module_PVTwin_inkl_forside.pdf> (last accessed on January 2016).
[59] Canadian centre for housing technology, <http://www.ccht-cctr.gc.ca> (last accessed on January 2016).
[60] M. Armstrong, Personal Communication, Canadian Centre for Housing Technology, Ottawa, Canada, 2011.
[61] I. Knight, H. Ribberink, European and Canadian non-HVAC Electric and DHW Load Profiles for use in Simulating the Performance of Residential Cogeneration Systems, IEA/ECBCS Annex 42 report, <http://www.ecbcs.org/annexes/annex42.htm> (last accessed on March 2015).
[62] EnergyPlus, Weather data, EnergyPlus Energy Simulation Software, U.S. Department of Energy, <http://apps1.eere.energy.gov/buildings/energyplus/> (last accessed on January 2016).
[63] H. Demuth, M. Beale, M. Hagan, Network ToolboxTM 6, User's Guide.
[64] National Inventory Report 1990-2012: Greenhouse Gas Sources and Sinks in Canada - Executive Summary, 2014, <http://ec.gc.ca/Publications/default.asp?lang=En&xml=BF55E9F2-EDD6-4AEB-B804-004C39BDC712> (last accessed on August 2016).
[65] Independent Electricity System Operator (IESO), <http://www.ieso.ca/> (last accessed on August 2016).

[66] Sustainable Energy Authority of Ireland (SEAI), <http://www.seai.ie/Your_Business/Public_Sector/FAQ/Calculating_Savings_Tracking_Progress/What_are_the_conversion_factors_used_to_calculate_TPER.html> (last accessed on August 2016).
[67] G. Chicco, P. Mancarella, Assessment of the greenhouse gas emissions from cogeneration and trigeneration systems. Part I: models and indicators, Energy 33 (2008) 410–417.
[68] A. Hawkes et al., Impact of Support Mechanisms on Microgeneration Performance in OECD Countries, published by Technische Universität München, Germany, 10/2014, <http://www.iea-ebc.org/fileadmin/user_upload/docs/Annex/EBC_Annex_54_Micro-Generation_Support_Mechanisms.pdf> (last accessed on February 2016).

Please cite this article in press as: E. Entchev et al., Energy, economic and environmental performance simulation of a hybrid renewable microgeneration system with neural network predictive control, Alexandria Eng. J. (2016), http://dx.doi.org/10.1016/j.aej.2016.09.001